

# 1 Particle - 1 Qubit: Particle Physics Data Encoding for Quantum Machine Learning

Aritra Bal\* and Markus Klute  
*Institute of Experimental Particle Physics (ETP),  
 Karlsruhe Institute of Technology, Karlsruhe, DE*

Benedikt Maier,<sup>†</sup> Melik Oughton, and Eric Pezone  
*Imperial-X and Department of Physics, Imperial College Of Science, Technology And Medicine, London, UK*

Michael Spannowsky<sup>‡</sup>  
*Institute for Particle Physics Phenomenology (IPPP), Durham University, Durham, UK*  
 (Dated: February 25, 2025)

We introduce 1P1Q, a novel quantum data encoding scheme for high-energy physics (HEP), where each particle is assigned to an individual qubit, enabling direct representation of collision events without classical compression. We demonstrate the effectiveness of 1P1Q in quantum machine learning (QML) through two applications: a Quantum Autoencoder (QAE) for unsupervised anomaly detection and a Variational Quantum Circuit (VQC) for supervised classification of top quark jets. Our results show that the QAE successfully distinguishes signal jets from background QCD jets, achieving superior performance compared to a classical autoencoder while utilizing significantly fewer trainable parameters. Similarly, the VQC achieves competitive classification performance, approaching state-of-the-art classical models despite its minimal computational complexity. Furthermore, we validate the QAE on real experimental data from the CMS detector, establishing the robustness of quantum algorithms in practical HEP applications. These results demonstrate that 1P1Q provides an effective and scalable quantum encoding strategy, offering new opportunities for applying quantum computing algorithms in collider data analysis.

## I. INTRODUCTION

The unprecedented collision energies achieved at latest- and next-generation colliders, like the Large Hadron Collider (LHC) and the Future Circular Collider (FCC), produce vast amounts of particle-level data, challenging the limits of conventional data analysis techniques in high energy physics (HEP). With the increasing complexity of these datasets, novel approaches that leverage cutting-edge computational paradigms have become indispensable. Quantum computing, with its ability to exploit superposition, entanglement, and interference, offers a promising framework to address some of the most intricate challenges in HEP.

In recent years, Machine Learning (ML) has established itself as an indispensable tool for analysing HEP data, leading to significant advancements in tasks such as event classification, anomaly detection, and parameter estimation. The next frontier in this field is to extend these techniques to the quantum domain, leveraging Quantum Machine Learning (QML) to enhance data analysis capabilities. Any quantum machine learning algorithm consists of three key components: (1) the data encoding, which maps classical data onto quantum states; (2) the quantum model, typically implemented through quantum circuits and quantum operations such as entanglement between qubits; and (3) the loss function,

whose optimization is crucial for training the quantum model. While substantial efforts have been devoted to designing quantum models and optimizing loss functions [1, 2], the choice of data encoding remains a critical yet underexplored aspect of QML for HEP applications. In this work, we propose a new encoding scheme tailored to HEP data, which we call 1P1Q (1 Particle - 1 Qubit). This encoding strategy assigns a separate qubit to each particle, enabling an efficient and direct representation of collider events without prior data compression.

We demonstrate the effectiveness of quantum machine learning models in processing HEP data by employing two distinct approaches: a Quantum Autoencoder (QAE) [3] for unsupervised, unlabelled learning and a Variational Quantum Circuit (VQC) [4] for classification tasks. Both methods fully exploit the kinematic information of particles encoded via the 1P1Q scheme, using the quantum state representation to retain and process intricate correlations that are often lost in classical compression techniques. The QAE compresses quantum states by learning a lower-dimensional latent representation, making it well-suited for anomaly detection in collider physics, while the VQC employs a parametrized quantum circuit to discriminate between different class categories based on learned quantum features.

We apply these quantum machine learning models to one of the most well-established use cases of classical machine learning in HEP: the discrimination of hadronically decaying resonances from the overwhelming background of QCD jets. Identifying such resonances, including those from top quarks, Higgs bosons, or hypothetical new physics states, is crucial for advancing our

\* aritra.bal@kit.edu

† benedikt.maier@cern.ch

‡ michael.spannowsky@durham.ac.uk

understanding of fundamental interactions. We find that for this task, VQC and QAE models acting on 1P1Q-encoded particle information result in highly performant QML algorithms, equal to or even better than comparable classical counterparts in the case of the QAE.

Compared to existing approaches [5–9], which first encode the information of the collider events into an abstract, typically compressed, latent representation using classical machine learning algorithms or domain-inspired high-level features, 1P1Q provides more immediate access to the raw information of collider events and allows for the direct exploitation of their content using quantum variational circuits. This has two main benefits: First, classical neural network architectures may result in a lossy representation and not fully capture the raw event content. Second, and related, 1P1Q provides a natural way of extending the input space as quantum computers and their simulators can accommodate more and more qubits.

For the first time, our study explores QML in HEP using actual experimental data recorded by the CMS detector in 2016. This real-world application provides a critical test of the robustness and feasibility of QML strategies beyond simulated datasets. By demonstrating that QML models can be trained on and extract meaningful physics from real collision events, we show that 1P1Q can become a promising, lossless collider data encoding framework as quantum computing hardware advances.

In this paper, we present the formulation of the 1P1Q encoding, explore its theoretical underpinnings, and discuss its potential applications to jet physics at the LHC and future colliders with the examples of anomaly detection and a supervised classifier. We demonstrate how this encoding captures the essential kinematic features of jets and showcase its utility in leveraging quantum algorithms to analyze jet substructure, and compare to state-of-the-art classical machine learning algorithms.

## II. 1P1Q - PARTICLE ENCODING

In collider measurements, reconstructed particles are kinematically fully described by three key parameters: the transverse momentum  $p_T = \sqrt{p_x^2 + p_y^2}$ , where  $p_x$  and  $p_y$  are the momentum components in the transverse detector plane, the pseudorapidity  $\eta$ , and the azimuthal angle  $\phi$ . The pseudorapidity  $\eta$  is related to the polar angle  $\nu$  of the particle’s trajectory by  $\eta = -\ln \tan(\nu/2)$ , which provides an approximation of the rapidity in high-energy regimes. Finally, the azimuthal angle  $\phi$  describes the particle’s direction in the transverse plane and is measured relative to a chosen reference axis. Together, these three quantities specify the particle’s momentum.

The 1P1Q method directly encodes the kinematics of a particle on a qubit. The pseudorapidity  $\eta$  and the azimuthal angle  $\phi$  of the particle, modulated by the transverse momentum  $p_T$  normalized to the  $p_T$  of the jet, are

used as spherical coordinates on the Bloch sphere to orient the qubit, enabling a compact and information-rich representation of each particle as a quantum state that is not dependent on the energy scale of the jet, thus facilitating a straightforward transition to the quantum domain. These feature encodings, represented by rotation angles about the  $Y$  and  $X$  axes respectively, are then additionally scaled by a factor  $f = f(w)$  constrained to lie between  $[1, 2\pi + 1]$ , where  $w$  is a trainable parameter. This ensures the particles can spread out across the Bloch sphere instead of clustering too closely around its North Pole. This is especially true when using normalized  $p_T$  distributions, where each particle  $p_T$  gets normalized by the jet  $p_T$  and thus tends to have small values, as can be seen in Figure 1, where we show the effect of this scaling for the ten hardest particles from a  $QCD$  jet and a jet produced from a top quark decay. The encoding can then be summarized as:

$$f \cdot \frac{p_T}{p_{T,\text{jet}}} \cdot (\eta - \eta_{\text{jet}}) \rightarrow \theta \quad (1)$$

$$f \cdot \frac{p_T}{p_{T,\text{jet}}} \cdot (\phi - \phi_{\text{jet}}) \rightarrow \varphi \quad (2)$$

$$(p_T, \eta, \phi) \rightarrow |\psi\rangle = R_X(\varphi)R_Y(\theta)|0\rangle \\ = \alpha(\theta, \varphi)|0\rangle + \beta(\theta, \varphi)|1\rangle \quad (3)$$

$$f \rightarrow 1 + \frac{2\pi}{1 + e^{-w}} \quad (4)$$

In the above equations, we take the coordinates  $\eta$  and  $\phi$  relative to the jet axis. While LHC collisions can result in hundreds of final-state particles, we limit our studies to the intrinsic structure of jets rather than entire events due to the limitations of currently available quantum computers and their simulators. Studying the substructure of jets can be a very powerful way to disentangle boosted, hadronically decaying electroweak-scale or beyond-the-standard-model resonances from QCD-induced jets [10]. Furthermore, in order to allow for efficient simulation of our quantum circuits on a simulator, we limit our study by using up to ten hardest jet constituents, which are expected to carry most of the information relevant to jet substructure analysis. Fig. 1 shows an example of the encoding for the ten hardest particles in a top-decay event (red) and a QCD light-flavour jet event (blue). Each particle is encoded on a different qubit. The scaling factor in Eq. 4 increases the angles on the Bloch sphere.

## III. QUANTUM CIRCUITS FOR ANOMALY DETECTION AND CLASSIFICATION

Anomaly detection is pivotal in high-energy physics, where new physics signatures often manifest as deviations from Standard Model predictions. The vast data volumes and model-agnostic nature of potential signals

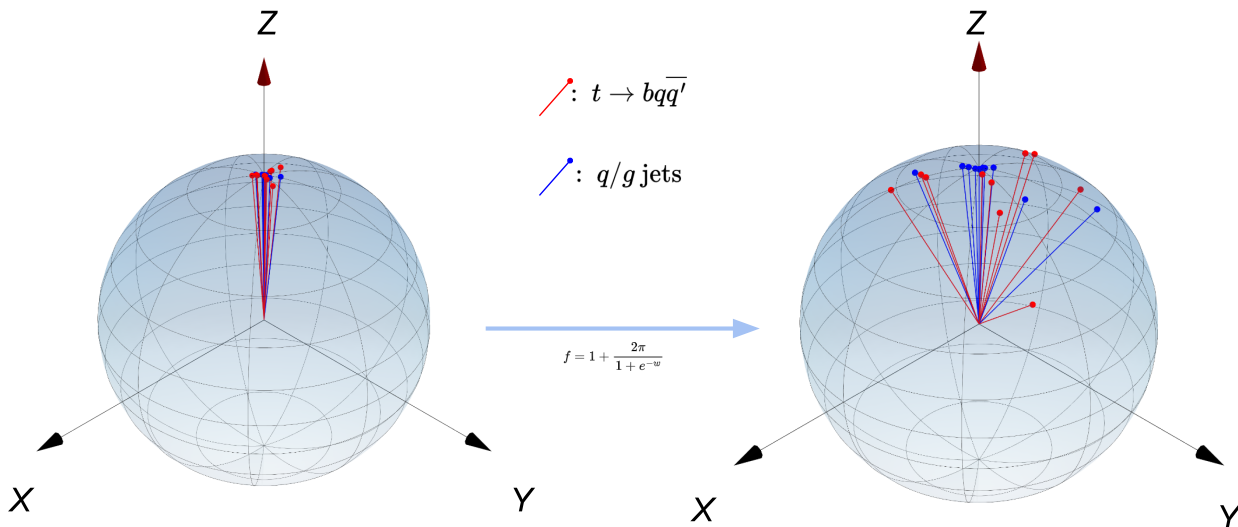


FIG. 1: Bloch Sphere: Effect of the input scaling described in Equation 4 when applied to the ten hardest particles of a QCD and top jet with comparable jet  $p_T$ . The value of  $w$  converges to a scaling factor  $f = 7.268$  for the VQC.

require robust detection methods. In classical machine learning, unsupervised learning models such as autoencoders have emerged as efficient tools for anomaly detection [11]. These work by compressing the input data into a latent space and reconstructing it, highlighting anomalous events through elevated reconstruction errors.

Quantum autoencoders (QAEs) extend this paradigm to quantum devices [3]. A QAE consists of an encoder and a decoder implemented via variational quantum circuits. The encoder compresses the input quantum state into a smaller latent representation, discarding qubits as necessary. The decoder then reconstructs the input from this latent state using the Hermitian conjugate of the encoding operators. Without sufficient dimensionality reduction in the latent space, a network would be able to learn the identity transformation trivially. Unlike classical autoencoders, QAEs perform this reduction by replacing the discarded qubits (hereafter referred to as trash states) with reference states that are initialized to  $|0\rangle$ , thus creating an information bottleneck. Naturally, this would require the number of trash states  $N_{\text{trash}}$  and reference states  $N_{\text{ref}}$  to be equal.

The unitary transformations within a QAE consist of a combination of parameterized single-qubit rotations and multi-qubit entangling gates, such as the Controlled NOT (CNOT) gate. To demonstrate its applicability to the task of anomaly detection, we use the procedure described in Equations 1 and 2, to encode information into our quantum circuit. Next, to allow the network to learn

higher-order non-linear terms, we entangle all possible pairs of qubits using two-qubit CNOT gates. For a system of  $N$  qubits, this would require a total of  $N(N-1)/2$  operations. Finally, to ensure the network learns an optimal representation of the input space, we apply three parameterized rotations, one along each axis to each qubit. These trainable parameters are optimized using the classical Adam Optimizer [12], with a scheduler that periodically decays the learning rate. The entanglement and rotation operations are summarized in Equation 5.

$$U(\Theta) = \left( \bigotimes_{i=1}^N R_X(\phi_i) R_Z(\theta_i) R_Y(\omega_i) \right) \otimes \left( \bigotimes_{1 \leq i < j \leq N} C_{ij} \right). \quad (5)$$

The quantum circuits presented in this study are simulated and optimized using the Quantum Machine Learning library `pennylane` [13] with the `lightning.gpu` and `lightning.kokkos` devices. To train the QAE, we seek to maximize the fidelity between the output and input states in the subspace relevant for reconstruction. Using an equivalent approach first introduced in [14], we minimize instead the cost function defined as the negative of the fidelity between the trash and reference states. This fidelity measurement is performed using a SWAP test [15], which requires an ancillary qubit initialized to  $|0\rangle$ .

Using specific examples, QAEs have shown first successes compared to classical AEs regarding training efficiency and performance. The QAE of [3] requires fewer

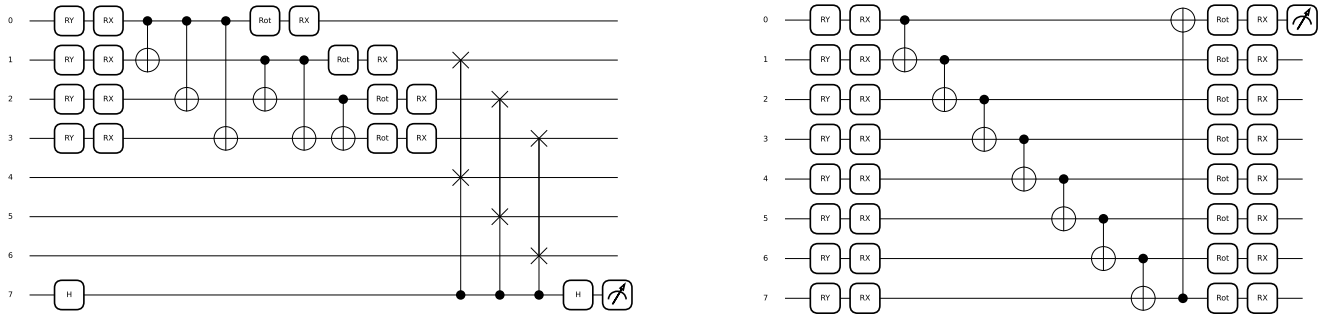


FIG. 2: QAE Circuit (left) used for anomaly detection. VQC (right) used for supervised classification. Example circuits with 4 and 8 input particles, respectively.

training samples to converge and generally outperforms CAEs in anomaly detection tasks.

In addition to its applicability for as an anomaly detection tool, we demonstrate that the 1P1Q encoding can just as well be used for classification within a supervised learning paradigm. For this task, we use a Variational Quantum Classifier (VQC) that learns to separate signal and background classes [4], in this case jets initiated by top quarks decaying hadronically versus jets initiated by light quarks or gluons.

The VQC is similar to the encoder of the QAE, with features being first encoded into the circuit using the procedure outlined in Equations 1-4. This is followed by entanglement operations using two-qubit CNOT gates between adjacent qubits, to allow for the introduction of non-linear terms into the network. For an input space of  $N$  qubits, this would require  $N + 1$  CNOT operations. Lastly, three trainable rotation gates are applied to each qubit, which allows the network to learn an optimal representation that separates signal from background, as summarized in Equation 6. Unlike the autoencoder, which is optimized by maximizing the fidelity between the trash and reference states, the VQC is optimized by performing a measurement of the expectation value of the Pauli  $Z$  observable on a target qubit, usually the first qubit, which is bounded in  $[-1, 1]$ . The final prediction from the VQC (Equation 7) is arrived at by adding a classical bias term, also a trainable parameter, to this expectation value. The circuit optimization is performed using the Mean Squared Error (MSE) between the prediction and the truth label as the loss function, along with the Adam Optimizer. The complete VQC circuit is shown in Figure 2 for an input of  $N = 8$  particles.

$$U(\Theta) = \left( \bigotimes_{i=1}^{N-1} R_X(\phi_i) R_Z(\theta_i) R_Y(\omega_i) \right) \otimes \left( \bigotimes_{i=0}^N C_{i,(i+1) \bmod N} \right) \quad (6)$$

$$f(x) = \langle q(x) | Z | q(x) \rangle + b \quad (7)$$

We highlight that for an input space comprising of the  $N$  hardest input particles per jet, the QAE requires only  $3N + 1$  trainable parameters to learn a suitable reconstruction of the inputs. Likewise, the VQC requires only  $3N + 2$  parameters.

#### IV. TRAINING DATASETS

The JETCLASS dataset introduced in [16], is a vast library containing 100M jets for training, 5M jets for validation and 20M jets for inference respectively, equally divided into ten classes. For the purpose of training our QAE, we use jets initiated by light quarks or gluons, hereafter referred to as the *background* jets. Such jets are produced in abundance at the LHC. Inference is then performed on both background as well as signal jets, comprising jets produced by decays of particles such as the Higgs,  $W$  or  $Z$  bosons, or the top quark. Since the QAE is trained to reconstruct only jets initiated by light quarks or gluons, we expect this reconstruction quality, defined as the fidelity between the trash and reference states described in Section III, to differ between signal and background, thus providing a degree of separation.

$$F = \sum_{i=1}^{N_{\text{ref}}} \langle T_i | R_i \rangle \quad \forall \quad T_i \in H^T, R_i \in H^{\text{ref}} \quad (8)$$

For training the QAE and VQC respectively, we first sample jets such that each class has a flat distribution in jet  $p_T$ , in the range  $[500, 1000]$  GeV, so as to not bias the training towards the scale of the jet, allowing us to purely focus on jet substructure.

We also demonstrate the effectiveness of our encoding for anomaly detection by training the QAE on real world data, recorded with the CMS Detector at the LHC [17] in 2016. This dataset, recently released in a machine-learning friendly format [18] is dominated by QCD jets, with contamination from other sources being estimated at less than 1% overall.

## V. RESULTS AND BENCHMARKING

### A. Quantum Autoencoder

The QAE is an example of an unsupervised learning algorithm, since it does not require labelled data and can be trained only on the background class, which in this case comprises jets initiated by light quarks or gluons. We use a total of 10000 events for training and 2500 events for validation. Inference is performed on 10000 events of each of the following class of events:  $H \rightarrow b\bar{b}$ ,  $H \rightarrow c\bar{c}$ ,  $H \rightarrow gg$ ,  $W \rightarrow q\bar{q}$ ,  $Z \rightarrow q\bar{q}$  and  $t \rightarrow bq\bar{q}'$ . The signal jets are also sampled to have a flat  $p_T$  distribution in the range [500, 1000] GeV.

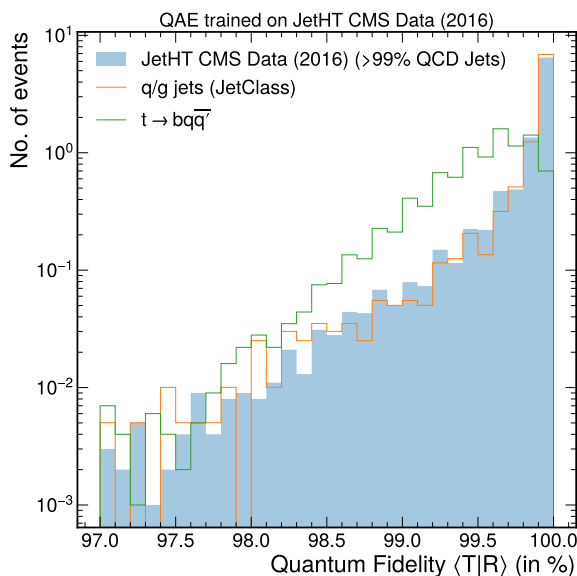


FIG. 3: Quantum Fidelity distributions for a system with 10 input qubits and a latent space of 2 qubits

We train the QAE on two different sets: simulated QCD jets from the JetClass dataset, and the real jet data recorded with the CMS Detector in 2016. Figure 3 shows that a QAE trained on data is comparable in performance to one trained on simulated events, when applied to the task of differentiating between simulated QCD events and simulated signal models.

For the first time, to our knowledge, we also show the results in Figure 3 of using a quantum machine learning algorithm with CMS open data to prove that the QAE can learn the underlying physics of the jet and is not biased by the detector response.

Figure 4 illustrates the AUC scores as a function of the quantum fidelity metric  $\langle 1 - \text{Fidelity} \rangle_{\text{QCD}}$  for different quantum autoencoder (QAE) configurations trained on either simulated JetClass QCD jets (dashed lines) or real CMS data (dotted lines). The three panels correspond to different input sizes, namely 6, 8, and 10 jet

constituents, while different marker shapes indicate varying latent space sizes. Across all configurations, higher AUC scores correlate with increased  $\langle 1 - \text{Fidelity} \rangle_{\text{QCD}}$ , indicating that the fidelity loss serves as a useful proxy for anomaly detection performance. The performance is particularly strong for top quark jets ( $t \rightarrow bq\bar{q}'$ , red), which consistently achieve the highest AUC scores, followed by Higgs decays to bottom quarks ( $H \rightarrow b\bar{b}$ , blue). The similarity in trends between models trained on real and simulated data highlights the robustness of the QAE in learning fundamental jet substructure features independent of dataset origin. Additionally, larger input sizes tend to improve performance, suggesting that incorporating more jet constituents provides richer representations for classification.

To benchmark the performance of the 1P1Q-encoded QAE against a classical counterpart, we trained on simulated QCD jets and considered as anomalies to this background the signals of hadronic  $W$  boson, Higgs boson and top quark decays. While the QAE has a simple structure of 10 input qubits, followed by the circuit of Figure 2 (left) and a latent space of 2, the classical autoencoder (CAE) model is allowed to be significantly larger, consisting of an encoder model containing an input feature vector of size 30, to be able to encode the same number of features encoded on the QAE, followed by dense layers of size 20 – 16 – 12 and a latent space 6. The decoder of the CAE has an identical, yet inverse, structure.

The QAE achieves superior performance compared to the CAE across all signal types. The QAE maintains this advantage despite having only 32 trainable parameters, in contrast to the CAE’s 2,500 parameters, demonstrating the potential of quantum machine learning to capture relevant physics with a significantly reduced model complexity efficiently.

Algorithm	Signals		
	$W \rightarrow q\bar{q}$	$H \rightarrow b\bar{b}$	$t \rightarrow bq\bar{q}'$
QAE	0.693	0.757	0.861
CAE	0.671	0.739	0.858

TABLE I: AUC scores QAE vs CAE: trained on a 10-particle input space

### B. Variational Quantum Circuit

For the supervised classification task, we employ the VQC to distinguish jets originating from top quark decays ( $t \rightarrow bq\bar{q}'$ ) from those initiated by light quarks or gluons. The VQC is trained using 1,000 events and validated on 500 events, with an inference dataset of 10,000 events equally distributed between signal and background classes, with all jets sampled to have a flat  $p_T$  distribution.

Figure 4 presents the Receiver Operating Characteristic (ROC) curves comparing the VQC trained on the

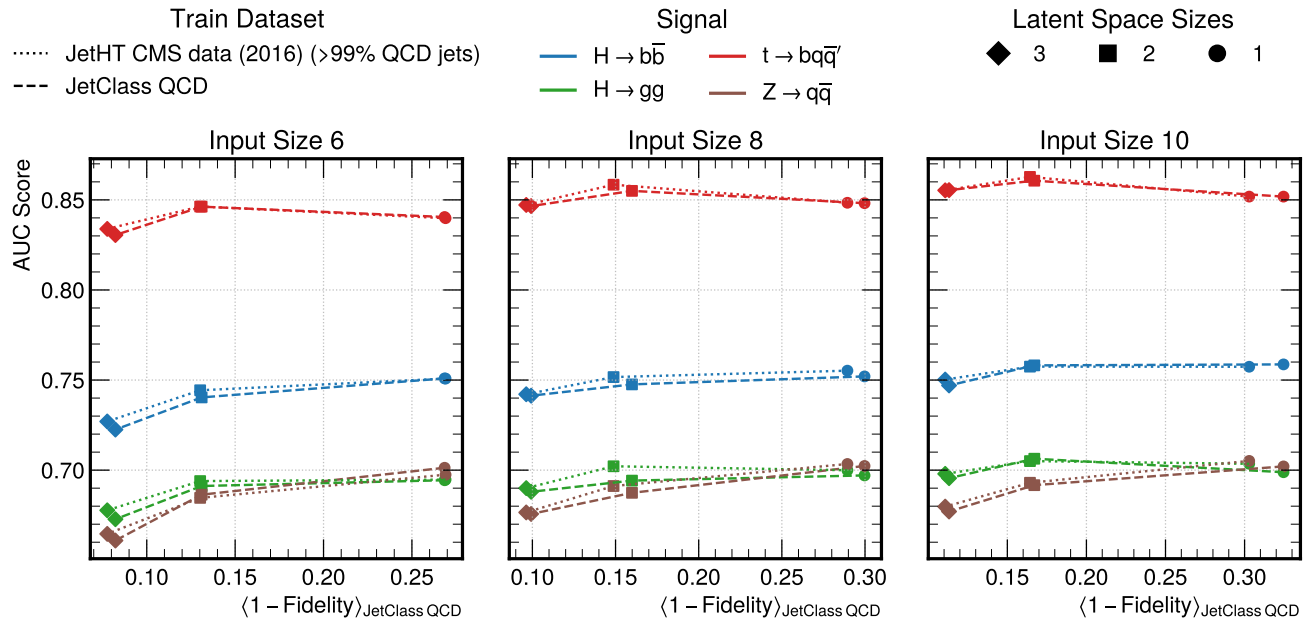


FIG. 4: AUC scores vs.  $\langle 1 - \text{Fidelity} \rangle_{\text{QCD}}$  for different QAE configurations. Models trained on simulated (dashed) and real CMS data (dotted) show consistent trends, with larger input sizes and higher fidelity loss correlating with improved anomaly detection performance.

1P1Q-encoded dataset against the state-of-the-art Particle Transformer (ParT) classifier[19], both trained using the 10 hardest particles per jet, and the same number of jets. The ROC curve demonstrates that the VQC achieves strong classification performance, with an AUC score of 0.876. Although the Particle Transformer model achieves a slightly higher AUC of 0.898, the VQC remains competitive despite having significantly fewer trainable parameters (32 vs. over 2 million). Furthermore, at a signal efficiency of 99%, the VQC achieves a background rejection of  $\text{REJ99} = 2.288$ , outperforming the Particle Transformer’s  $\text{REJ99} = 2.048$ .

This result shows the efficiency and potential of quantum machine learning models in jet classification tasks, especially when using the 1P1Q particle encoding. Such a quantum machine learning method offers competitive performance to classical state-of-the-art frameworks with drastically reduced computational resources.

### C. 1P1Q encoding

As detailed in Section I, quantum machine learning methods consist not only of the models, such as QAE or VQC, but also of the encoding step that maps classical data onto a quantum device. Both components jointly define the expressivity and efficiency of a quantum machine learning approach. Thus, to assess the QAE and VQC models’ ability to utilize the information provided by the 1P1Q data encoding, we successively reduce the features encoded on each qubit and observe the resulting

performance degradation.

Algorithm	Inputs	$(p_T, \eta, \phi)$	$(p_T, \eta)$	$(\eta, \phi)$	$(p_T, \phi)$
	VQC		<b>0.876</b>	0.846	0.805
QAE		<b>0.861</b>	0.813	0.791	0.804

TABLE II: AUC scores vs Input Features for the VQC and QAE, for the benchmark signal:  $t \rightarrow bq\bar{q}'$

Table II shows the impact of different input feature combinations within the 1P1Q encoding scheme on classification performance. The best AUC scores are achieved when all three features  $(p_T, \eta, \phi)$  are included, suggesting that the full kinematic variables contribute significantly to the model’s performance. When one feature is removed, we observe a performance drop, with the most pronounced reduction occurring when  $p_T$  is excluded. This emphasizes the importance of transverse momentum information in jet classification tasks and suggests that quantum models are particularly effective at utilizing correlations between momentum and angular variables. The robustness of these results across different models further validates the suitability of 1P1Q encoding for high-energy physics applications.

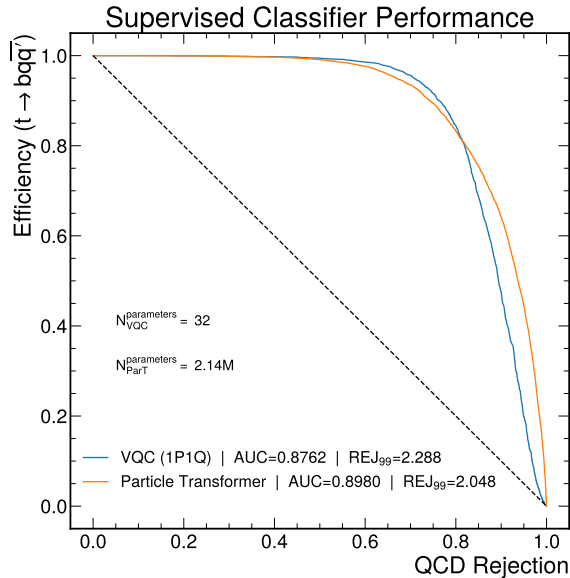


FIG. 5: Comparison of ROC curves for the VQC and Particle Transformer. The VQC trained on the 1P1Q-encoded dataset closely matches the performance of the state-of-the-art Particle Transformer, despite using significantly fewer trainable parameters, with both being trained on the same number of events and input size of 10 particles.

## VI. SUMMARY

In this work, we introduced the 1P1Q encoding scheme, a novel approach for representing particle physics data on quantum hardware by assigning each particle to a separate qubit. This encoding allows direct utilization of raw collision event data without classical compression, enhancing the potential expressivity and efficiency of QML models. We demonstrated the effectiveness of this approach using two quantum machine learning models: a QAE for anomaly detection and a VQC for supervised classification. These models were trained on both

simulated and real experimental data, establishing the robustness of quantum algorithms in high-energy physics applications.

Our results show that the QAE successfully differentiates signal jets from background QCD jets, achieving superior performance compared to its classical counterpart while requiring significantly fewer trainable parameters. Furthermore, the VQC exhibits strong classification capability, approaching the performance of state-of-the-art classical models despite its minimal parameter count. By systematically reducing the encoded features, we established that the 1P1Q encoding effectively captures jet substructure information, and performance degradation with reduced feature input underscores the importance of a comprehensive quantum data representation.

For the first time, we validate a quantum machine learning model trained on real experimental data from the CMS detector, demonstrating that quantum approaches can extract meaningful physics insights in a real-world setting. These results establish the 1P1Q encoding as a viable and scalable data representation framework for quantum computing applications in particle physics. As quantum hardware continues to advance, the efficiency of the 1P1Q approach is tailored for more intricate and large-scale QML applications in high-energy physics, offering new perspectives for jet classification, anomaly detection, and beyond.

## ACKNOWLEDGEMENTS

The authors acknowledge the support of Schmidt Sciences, the Alexander von Humboldt Foundation, and IPPP, as well as the usage of computing resources on the TOpAS GPU cluster at the Scientific Computing Centre (SCC) KIT, and the RCS Cluster at Imperial College London. The authors also thank the NHR Center Karlsruhe for providing access to computing resources on the high-performance computer HoreKa, which is jointly supported by the German Federal Ministry of Education and Research (BMBF) and the state governments.

- 
- [1] S. Abel, J. C. Criado, and M. Spannowsky, Completely quantum neural networks, *Phys. Rev. A* **106**, 022601 (2022), arXiv:2202.11727 [quant-ph].
  - [2] S. Abel, A. Blance, and M. Spannowsky, Quantum optimization of complex systems with a quantum annealer, *Phys. Rev. A* **106**, 042607 (2022), arXiv:2105.13945 [quant-ph].
  - [3] V. S. Ngairangbam, M. Spannowsky, and M. Takeuchi, Anomaly detection in high-energy physics using a quantum autoencoder, *Phys. Rev. D* **105**, 095004 (2022), arXiv:2112.04958 [hep-ph].
  - [4] A. Blance and M. Spannowsky, Quantum Machine Learning for Particle Physics using a Variational Quantum Classifier, *JHEP* **02**, 212, arXiv:2010.07335 [hep-ph].
  - [5] A. Blance and M. Spannowsky, Unsupervised event classification with graphs on classical and photonic quantum computers, *JHEP* **21**, 170, arXiv:2103.03897 [hep-ph].
  - [6] V. Belis, K. A. Woźniak, E. Puljak, P. Barkoutsos, G. Dissertori, M. Grossi, M. Pierini, F. Reiter, I. Tavernelli, and S. Vallecorsa, Quantum anomaly detection in the latent space of proton collision events at the LHC, *Commun. Phys.* **7**, 334 (2024), arXiv:2301.10780 [quant-ph].

- [7] C. Duffy, M. Hassanshah, M. Jastrzebski, and S. Malik, Unsupervised Beyond-Standard-Model Event Discovery at the LHC with a Novel Quantum Autoencoder (2024), arXiv:2407.07961 [quant-ph].
- [8] A. Hammad, M. M. Nojiri, and M. Yamazaki, Quantum similarity learning for anomaly detection (2024), arXiv:2411.09927 [hep-ph].
- [9] V. Belis, P. Odagiu, M. Grossi, F. Reiter, G. Dissertori, and S. Vallecorsa, Guided quantum compression for high dimensional data classification, *Mach. Learn. Sci. Tech.* **5**, 035010 (2024), arXiv:2402.09524 [quant-ph].
- [10] S. Marzani, G. Soyez, and M. Spannowsky, *Looking inside jets: an introduction to jet substructure and boosted-object phenomenology*, Vol. 958 (Springer, 2019) arXiv:1901.10342 [hep-ph].
- [11] V. Chekhovsky *et al.* (CMS), Model-agnostic search for dijet resonances with anomalous jet substructure in proton-proton collisions at  $\sqrt{s} = 13$  TeV (2024), arXiv:2412.03747 [hep-ex].
- [12] D. P. Kingma and J. Ba, Adam: A method for stochastic optimization, in *3rd International Conference on Learning Representations, ICLR 2015, San Diego, CA, USA, May 7-9, 2015, Conference Track Proceedings*, edited by Y. Bengio and Y. LeCun (2015).
- [13] V. Bergholm, J. Izaac, M. Schuld, C. Gogolin, S. Ahmed, V. Ajith, M. S. Alam, G. Alonso-Linaje, B. Akash-Narayanan, A. Asadi, J. M. Arrazola, U. Azad, S. Banning, C. Blank, T. R. Bromley, B. A. Cordier, J. Ceroni, A. Delgado, O. D. Matteo, A. Dusko, T. Garg, D. Guala, A. Hayes, R. Hill, A. Ijaz, T. Isacsson, D. Ittah, S. Jhangiri, P. Jain, E. Jiang, A. Khandelwal, K. Kottmann, R. A. Lang, C. Lee, T. Loke, A. Lowe, K. McKiernan, J. J. Meyer, J. A. Montañez-Barrera, R. Moyard, Z. Niu, L. J. O’Riordan, S. Oud, A. Panigrahi, C.-Y. Park, D. Polatajko, N. Quesada, C. Roberts, N. Sá, I. Schoch, B. Shi, S. Shu, S. Sim, A. Singh, I. Strandberg, J. Soni, A. Száva, S. Thabet, R. A. Vargas-Hernández, T. Vincent, N. Vitucci, M. Weber, D. Wierichs, R. Wiersema, M. Willmann, V. Wong, S. Zhang, and N. Killoran, PennyLane: Automatic differentiation of hybrid quantum-classical computations (2022), arXiv:1811.04968 [quant-ph].
- [14] J. Romero, J. P. Olson, and A. Aspuru-Guzik, Quantum autoencoders for efficient compression of quantum data, *Quantum Science and Technology* **2**, 045001 (2017).
- [15] H. Buhrman, R. Cleve, J. Watrous, and R. de Wolf, Quantum fingerprinting, *Phys. Rev. Lett.* **87**, 167902 (2001).
- [16] H. Qu, C. Li, and S. Qian, Jetclass: A large-scale dataset for deep learning in jet physics, 10.5281/zenodo.6619768 (2022).
- [17] S. Chatrchyan *et al.* (CMS), The CMS Experiment at the CERN LHC, *JINST* **3**, S08004.
- [18] O. Amram, L. Anzalone, J. Birk, D. A. Faroughy, A. Hallin, G. Kasieczka, M. Krämer, I. Pang, H. Reyes-Gonzalez, and D. Shih, Aspen Open Jets: Unlocking LHC Data for Foundation Models in Particle Physics (2024), arXiv:2412.10504 [hep-ph].
- [19] H. Qu, C. Li, and S. Qian, Particle transformer for jet tagging, in *Proceedings of the 39th International Conference on Machine Learning*, Proceedings of Machine Learning Research, Vol. 162, edited by K. Chaudhuri, S. Jegelka, L. Song, C. Szepesvari, G. Niu, and S. Sabato (PMLR, 2022) pp. 18281–18292.